Synthesis of a novel visible light-driven and magnetically separable photocatalyst based on $BiFeO_3$-$YFeO_3$ type II heterojunction

Sofia M. Tikhanova [1], Mikhail P. Volkov [2], Ivan V. Buryanenko [3], Valentin G. Semenov [3,4], Zhandos Orazov [5], Valentin Romanovski [6,*], Vadim I. Popkov [1], Natalia A. Lomanova [7,*]

[1] Hydrogen Energy Laboratory, Ioffe Institute, St. Petersburg 194021, Russia

[2] Laboratory of Kinetic Phenomena in Solids at Low Temperatures, Ioffe Institute, St. Petersburg 194021, Russia

[3] RITVERC JSC, St. Petersburg 194223, Russia

[4] Mössbauer Spectroscopy Laboratory, Institute for Analytical Instrumentation of RAS, St. Petersburg 198095, Russia

[5] Center of Physical Chemical Methods of Research and Analysis, Al-Farabi Kazakh National University, Almaty 050040, Kazakhstan

[6] Department of Materials Science and Engineering, University of Virginia, Charlottesville 22904, USA

[7] Laboratory of New Inorganic Materials, Ioffe Institute, St. Petersburg 194021, Russia

* Corresponding author e-mail:

Valentin Romanovski: rvd9ar@virginia.edu

Natalia A. Lomanova: natus@mail.ioffe.ru

Table S1. Nominal and experimental chemical composition, crystallite and grain sizes of BFO-YFO samples

Sample	*x**(Y)	Key element ratio, Bi:Y:Fe***	Iron excess, δ_{Fe}***	Crystallite size, *d,* nm	Grain size**, μm
BFO	0.0	1.00:0.00:1.00	0.00	87	1.0
BYFO-01	0.1	0.91:0.09:1.02	0.02	25	0.30
BYFO-03	0.3	0.60:0.39:1.41	0.42	27	0.23
BYFO-04	0.4	0.43:0.57:1.53	0.53	50	0.20
BYFO-05	0.5	0.29:0.7:1.77	0.79	64	0.35
BYFO-06	0.6	0.21:0.59:1.51	0.89	46	0.67
BYFO-07	0.7	0.26:0.64:1.61	0.79	67	0.8
BYFO-09	0.9	0.08:0.92:1.29	0.29	49	1.3
YFO	1.0	0.00:1.00:1.00	0.00	71	2.1
Note: * - nominal value of x, ** - grain size was determined from SEM images. *** - key element ratio and iron excess were determined from EDXS results					

Table S2. Magnetic and photocatalytic characteristics of the BFO-YFO samples

Sample	Iron excess, δFe***	Magnetization *M*, emu/g (at 4 kOe)	Remnant magnetization, M_r, emu/g	Coercivity H_c, kOe
BFO	0.00	0.07	0.02	0.70
BYFO-01	0.02	0.47	0.06	0.17
BYFO-03	0.42	0.33	0.15	0.28
BYFO-04	0.53	2.40	0.92	0.39
BYFO-05	0.79	8.10	2.60	0.36
BYFO-06	0.89	8.20	3.20	0.40
BYFO-07	0.79	7.80	2.80	0.40
BYFO-09	0.29	2.60	1.00	0.37
YFO	0.00	0.01	1.00	23.00
Note: * - iron excess was determined from EDXS results				

Table S3. ^{57}Fe Mössbauer spectral parameters of the main phases of the BFO-YFO samples

Sample	Spectral component	Isomer shift (mm/s) ±0.02	Quadropole splitting (mm/s) ±0.03	Hyperfine field (T) ±0.3	Area (%) ±2	Phases [Ref.]
BFO	*Sextet*	0.40	-0.12	49.5	100	$BiFeO_3$ [37][36]
BYFO-05	*Doublet1*	0.37	1.80	-	3	$BiFeO_3$ [37][36]
	Doublet2	0.33	0.91	-	6	non-magnetic iron
	Sextet1	0.38	0.18	51.6	13	α-Fe_2O_3
	Sextet2	0.35	0.00	49.9	50	$YFeO_3$ [35][38]
	Sextet3	0.33	0.06	48.6	21	Fe_3O_4 (A)
	Sextet4	0.71	-0.09	46.3	7	Fe_3O_4 (B)
BYFO-09	*Doublet1*	0.32	0.70	-	2	$BiFeO_3$ [37][36]
	Doublet2	0.34	1.18	-	9	*am*-Fe_2O_3
	Sextet1	0.37	0.23	51.6	3	α-Fe_2O_3
	Sextet2	0.36	0.01	50.0	67	$YFeO_3$ [35][38]
	Sextet3	0.34	0.02	48.9	14	Fe_3O_4 (A)
	Sextet4	0.68	0.00	45.8	5	Fe_3O_4 (B)
YFO	*Sextet*	0.36	0.01	49.9	100	$YFeO_3$ [35][38]

Table S4. Theoretical and experimental parameters of the BFO-YFO samples' electronic structure

Sample	Phases	$E_{g\ Theor}$	$E_{g\ Calc}$	*x*	CB	VB	Ref. E_g	Ref. *x*
BFO	$BiFeO_3$	2.16	2.01	5.89	2.39	0.39	[9][4]	[6][14]
BYFO-01	$BiFeO_3$	2.16	2.02	5.89	2.40	0.38	[9][4]	[6][14]
BYFO-03	$BiFeO_3$	2.16	2.04	5.89	2.41	0.37	[9][4]	[6][14]
	o-$YFeO_3$	1.95	1.94	5.6	2.07	0.13	[5][13]	[7][15]
BYFO-04	$BiFeO_3$	2.16	2.04	5.89	2.41	0.37	[9][4]	[6][14]
	o-$YFeO_3$	1.95	1.91	5.6	2.05	0.15	[5][13]	[7][15]
BYFO-05	*o*-$YFeO_3$	1.95	1.91	5.6	2.06	0.14	[5][13]	[7][15]
BYFO-06	*o*-$YFeO_3$	1.95	1.84	5.6	2.02	0.18	[5][13]	[7][15]
BYFO-07	*o*-$YFeO_3$	1.95	1.85	5.6	2.02	0.18	[5][13]	[7][15]
BYFO-09	*o*-$YFeO_3$	1.95	1.86	5.6	2.03	0.17	[5][13]	[7][15]

YFO	*o*-$YFeO_3$	1.95	1.94	5.6	2.07	0.13	[5][13]	[7][15]

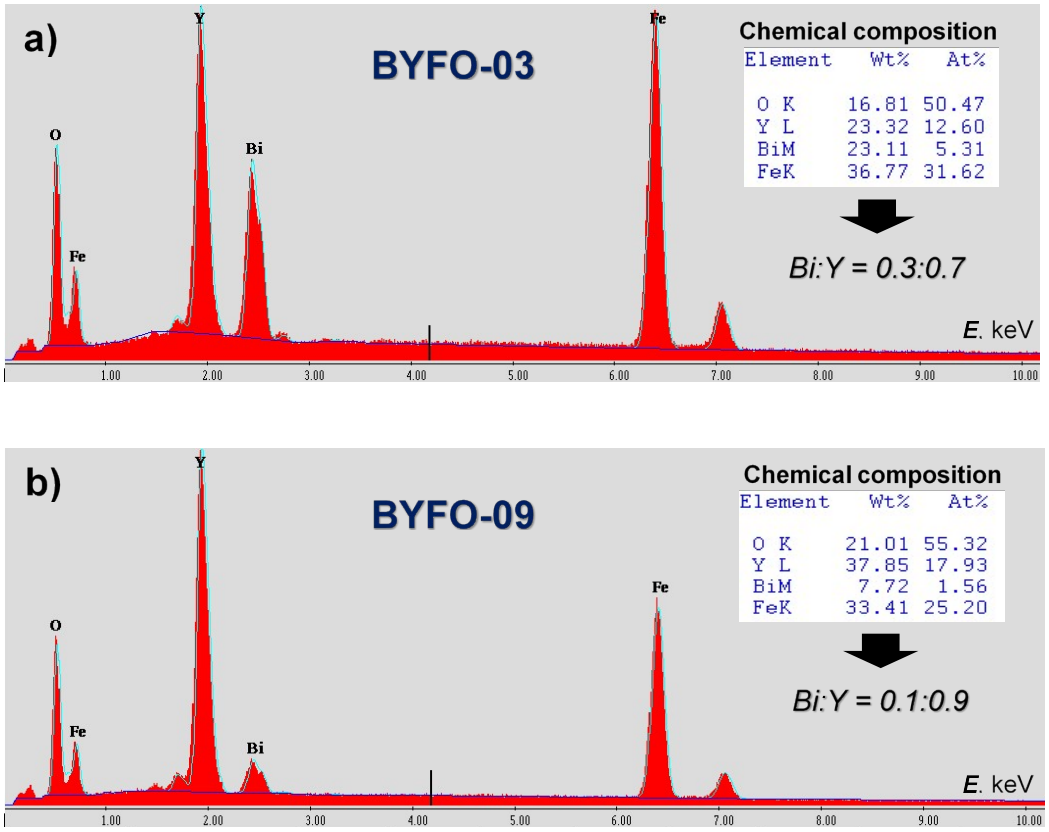

Fig. S1. EDX spectra of BYFO-03 (a) and BYFO-09 (b) samples.

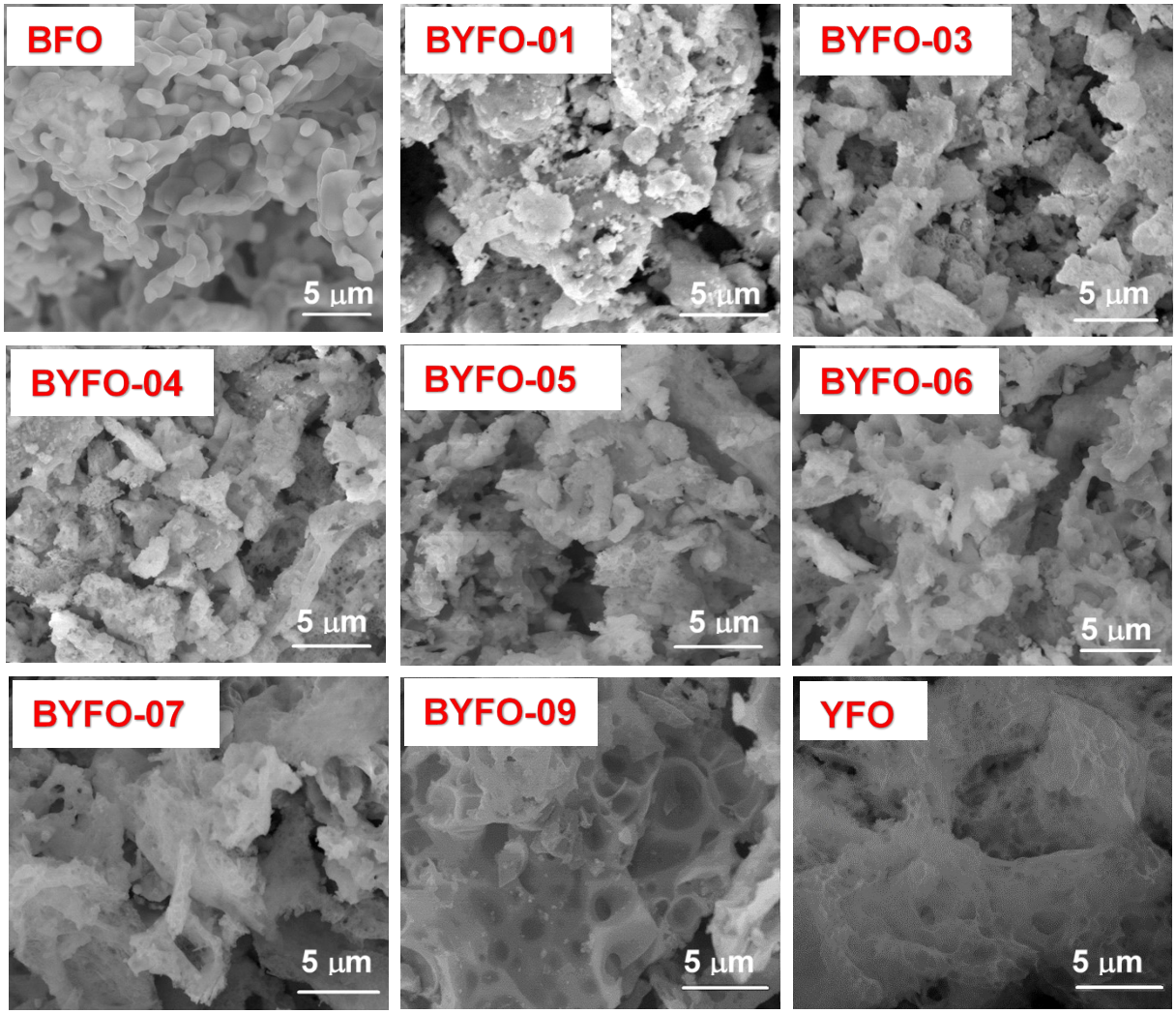

Fig. S2. SEM images of BFO, BYFO, and YFO samples.

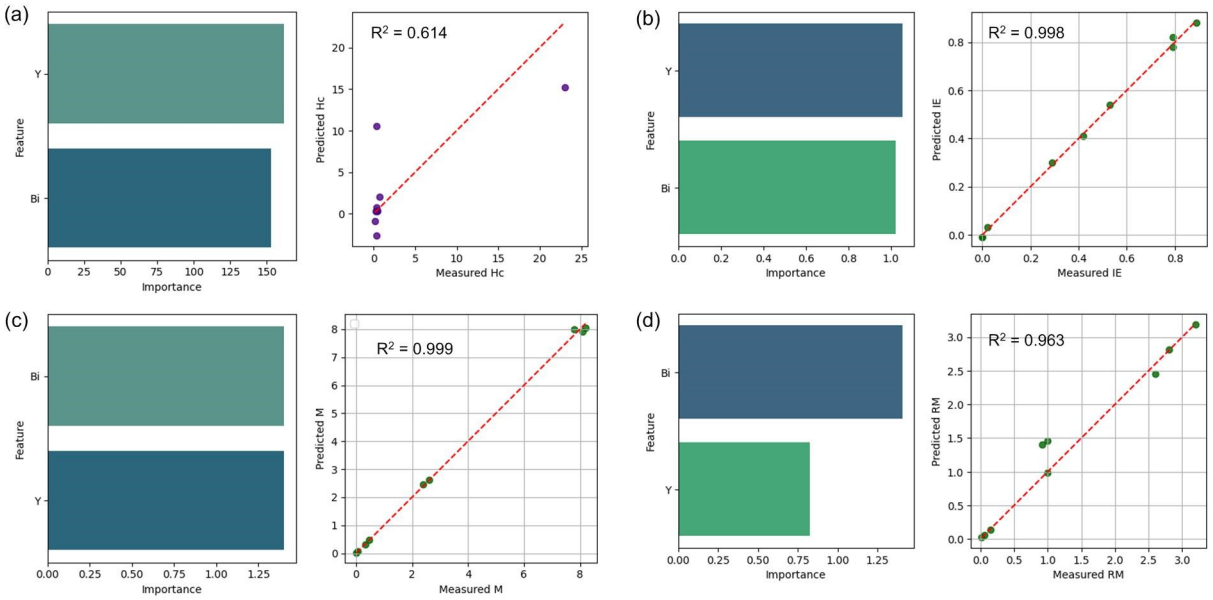

Fig. S3. Variable importance, and plots of predicted and measured values for Hc (a) - polynomial equation, IE (b) – SVR, M (c) – GPR, and RM (d) – SVR. Results for the best models are shown.

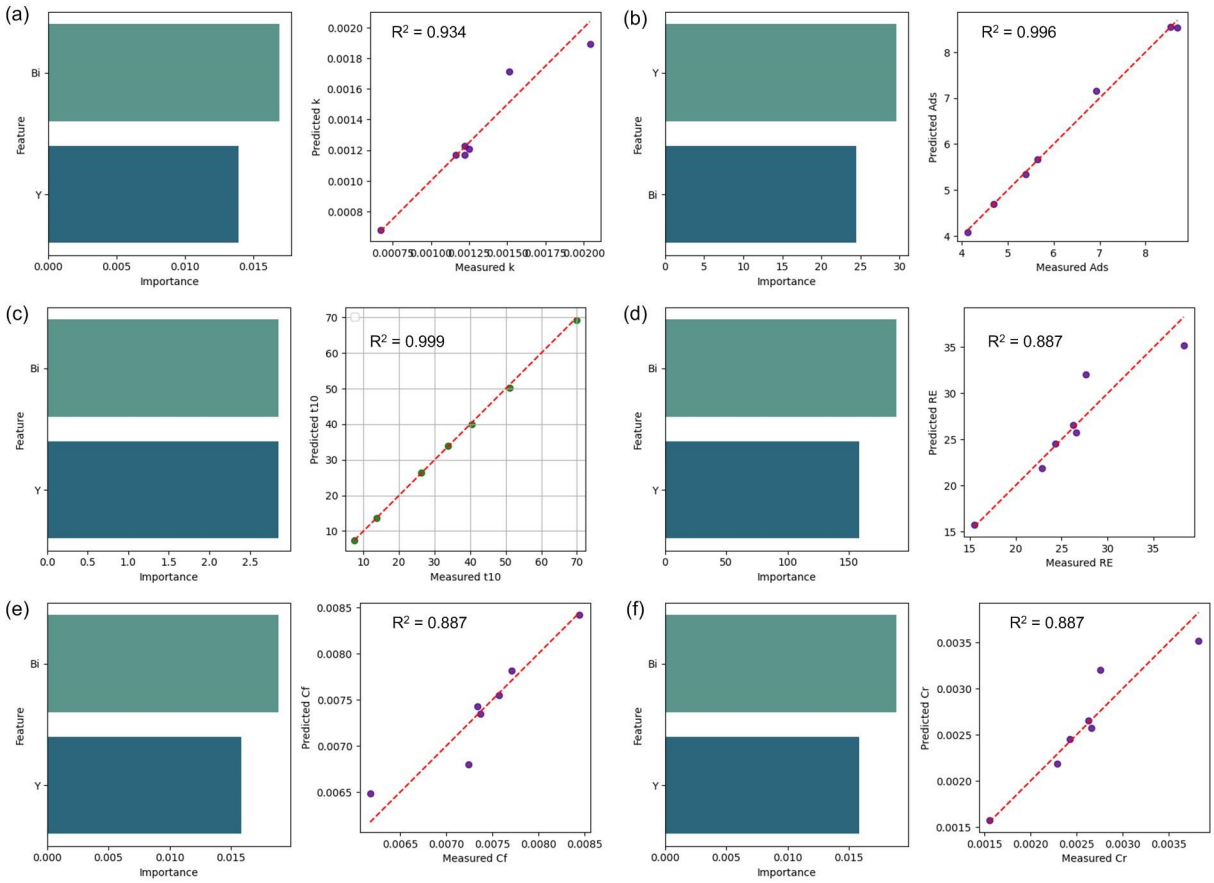

Figure S4. Variable importance, and plots of predicted and measured values for k (a) - polynomial equation, Ads (b) – polynomial equation, t_{10} (c) – GPR, RE (d) – polynomial equation, C_f (e) - polynomial equation, C_r (f) - polynomial equation. Results for the best models are shown.